Supplementary Information

Supplementary Table S1. Primer Sequences

Primer	Sequence	Source
AAE5NdeIkdsB	GAATTTAAACTAAAGTTTTGcatatgAGAAGAGCT GTAATCATACC [a]	Invitrogen
AAE3BamHIkdsB	GCCCCTGCGAGGAGCggatccAAGCTTATAAATTT TTTAACTTTTC [b]	Invitrogen
AAE5NdeIwaaA	ATATATATcatatgCAATTTGAAGTCCTGAAGAG [a]	Eurogentec
AAE3BamHIwaaA	ATATggatccTTAAAGACCTCTTAAAAACTCCCTA AG [b]	Eurogentec
HIN5NdeIwaaA	ATATATATcatatgTGGCGTTTTTTTTATACCAGCT [a]	Eurogentec
HIN3BamHIwaaA	ATATggatccTCATACATTGCGCTCCAAATAAGG [b]	Eurogentec
CPS5NdeIwaaA	ATATATATcatatgATCAAAGGTCGACGTAC [a]	Eurogentec
CPS3BamHIwaaA	TCTAGAggatccCTATATTTTTTACACAAGGG [b]	Eurogentec
ECO5NdeIwaaA	ATATATATcatatgCTCGAATTGCTTTACACCGC [a]	Eurogentec
ECO3BamHIwaaA	ATATggatccTCAATGCGTTTTCGGTGGCAG [b]	Eurogentec
ECOyrbG	CCACTGGCGTACAGTCGTGAC	Invitrogen
ECOkdsC	CCATCTGACAGTACGCCATCG	Invitrogen
ECOwaaCH1	AGCGCGTACTGGAAGAACTCAACGCGCTATTGT TACAAGAGGAAGCCTGAGTGTAGGCTGGAGCT GCTTC [c]	MWG
ECOwaaCH2	GATGATTTCAGAGTGTAAGGTTTCAATGAATGA AGTTTAAAGGATGTTAGCATATGAATATCCTCC TTAG [c]	MWG
ECOwaaAH1	ACAGCTAAATACATAGAATCCCCAGCACATCCA TAAGTCAGCTATTTACTGTGTAGGCTGGAGCTG CTTC [c]	MWG
ECOwaaAH2	TAATGGGATCGAAAGTACCCGGATAAATCGCCC GTTTTTGCATAACAACCCATATGAATATCCTCCT TAG [c]	MWG

[a] *Nde*I site is shown in lower case letters.

[b] *Bam*HI site is shown in lower case letters.

[c] Homology extension regions are underlined.

Supplementary Table S2. ESI FT-ICR MS Peak List of Unligated LPS Molecules Isolated from *A. aeolicus*

Molecule	Obs. Mass [a]	Calc. Mass	Chemical Composition [b]
M1	3211.67	3211.614	LA + 1*Hex, 3*HexA, 2*Hep, 1*Kdo
M2	4161.03	4160.978	LA + 2*Hex, 3*HexA, 1*HexNAc, 4*dHex, 2*Hep, 1*Kdo
M3	4323.10	4323.030	LA + 3*Hex, 3*HexA, 1*HexNAc, 4*dHex, 2*Hep, 1*Kdo
M4	1294.31	1294.329	1*Hex, 3*HexA, 2*Hep, 1*Kdo
M5	2243.70	2243.693	2*Hex, 3*HexA, 1*HexNAc, 4*dHex, 2*Hep, 1*Kdo
M6	2405.75	2405.745	3*Hex, 3*HexA, 1*HexNAc, 4*dHex, 2*Hep, 1*Kdo

[a] Mass numbers given refer to the monoisotopic masses of the neutral molecules deduced from the negative ion ESI FT-ICR mass spectra in Figure S2 of Supplemental Information.

[b] Abbreviations: LA, lipid A (calculated mass 1917.285 u); Hex, hexose; HexA, hexosuronic acid; HexNAc, *N*-acetyl hexosamine; dHex, deoxy-hexose; Hep, heptose; Kdo, 3-deoxy-D-*manno*-oct-2-ulosonic acid.

Supplementary Table S3. Sugar Composition of the LPS and the LPS Oligosaccharide (OS) Fraction of *A. aeolicus*

Component [a]	nmol/mg of LPS [b]	nmol/mg of OS [c]
Kdo_{AcP} [d]	0	1
Kdo_{HCl} [e]	27	58
Hep	50	98
GlcN	0	0
Gal	36	60
GalA	n.d. [f]	197
Rha	485	1537
Man	160	460
Glc	1306	2278

[a] Abbreviations: Kdo, 3-deoxy-D-*manno*-oct-2-ulosonic acid; Hep, heptose; GlcN, glucosamine; Gal, galactose; GalA, galacturonic acid; Rha, rhamnose; Man, mannose; Glc, glucose.

[b] Average of two analyses.

[c] Average of four analyses.

[d] Analysis of Kdo after mild hydrolysis in 0.1 M Na-acetate buffer, pH 4.4, at 100 °C for 1 h.

[e] Analysis of Kdo after strong hydrolysis in 1 M HCl at 100 °C for 2 h.

[f] Not determined.

Supplementary Table S4. ESI FT-ICR MS Peak List of LPS Molecules Isolated from *E. coli* Strains KPM123 and KPM124

Molecule	Obs. Mass [a]	Calc. Mass	Chemical Composition [b]
M1	1178.66	1178.661	2*GlcN, 2**P*, 3*14:0(3-OH)
M2	1398.72	1398.719	1*Kdo, 2*GlcN, 2**P*, 3*14:0(3-OH)
M3	1404.85	1404.854	2*GlcN, 2**P*, 4*14:0(3-OH)
M4	1624.91	1624.912	1*Kdo, 2*GlcN, 2**P*, 4*14:0(3-OH)
M5	1747.92	1747.921	1*Kdo, 2*GlcN, 2**P*, 1**P-EtN*, 4*14:0(3-OH)
M6	2027.15	2027.177	2*Kdo, 2*GlcN, 2**P*, 3*14:0(3-OH), 1*14:0[3-O(12:0)]
M7	2107.12	2107.143	2*Kdo, 2*GlcN, 3**P*, 3*14:0(3-OH), 1*14:0[3-O(12:0)]
M8	2237.35	2237.383	2*Kdo, 2*GlcN, 2**P*, 2*14:0(3-OH), 1*14:0[3-O(12:0)], 1*14:0[3-O(14:0)]
M9	2317.31	2317.349	2*Kdo, 2*GlcN, 3**P*, 2*14:0(3-OH), 1*14:0[3-O(12:0)], 1*14:0[3-O(14:0)]

[a] Mass numbers given refer to the monoisotopic masses of the neutral molecules deduced from the negative ion ESI FT-ICR mass spectra in Figure S3 of Supplemental Information.

[b] Abbreviations: GlcN, D-glucosamine; Kdo, 3-deoxy-D-*manno*-oct-2-ulosonic acid; *P*, phosphate; *P-EtN*, phosphoethanolamine; 14:0(3-OH), (*R*)-3-hydroxymyristate; 14:0[3-O(12:0)], dodecanoyloxytetradecanoyl unit attached to position 2′ of the non-reducing GlcN II; 14:0[3-O(14:0)], tetradecanoyloxytetradecanoyl moiety attached to position 3′ of GlcN II.

Supplementary Figure S1.

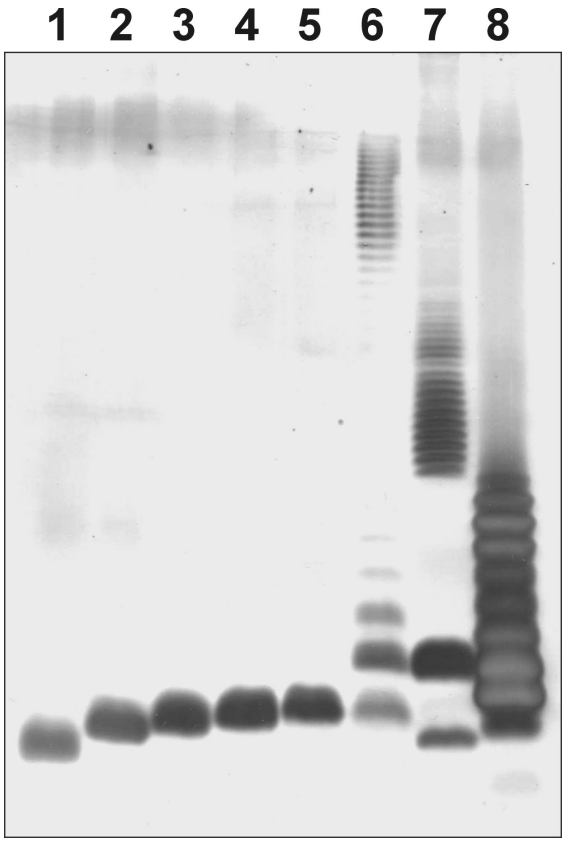

Supplementary Figure S1. SDS-PAGE analysis of the LPS profile of *A. aeolicus*. Proteinase K-digested whole-cell lysates of *A. aeolicus* and *S. enterica* sv. Typhimurium control strains, as well as purified LPS from *A. pyrophilus* (2 μg) (20) were separated on a 13% polyacrylamide gel and stained with silver nitrate. *Lane 1, S. enterica* sv. Typhimurium SL3769 (Rd1); *lane 2, S. enterica* sv. Typhimurium SL3748 (Rb3); *lane 3, S. enterica* sv. Typhimurium SL3750 (Rb2); *lane 4, S. enterica* sv. Typhimurium SL733 (Rb1); *lane 5, S. enterica* sv. Typhimurium SA1627 (Ra); *lane 6, S. enterica* sv. Typhimurium SL3770 (S-form LPS); *lane 7, A. aeolicus*; *lane 8, A. pyrophilus*.

Supplementary Figure S2.

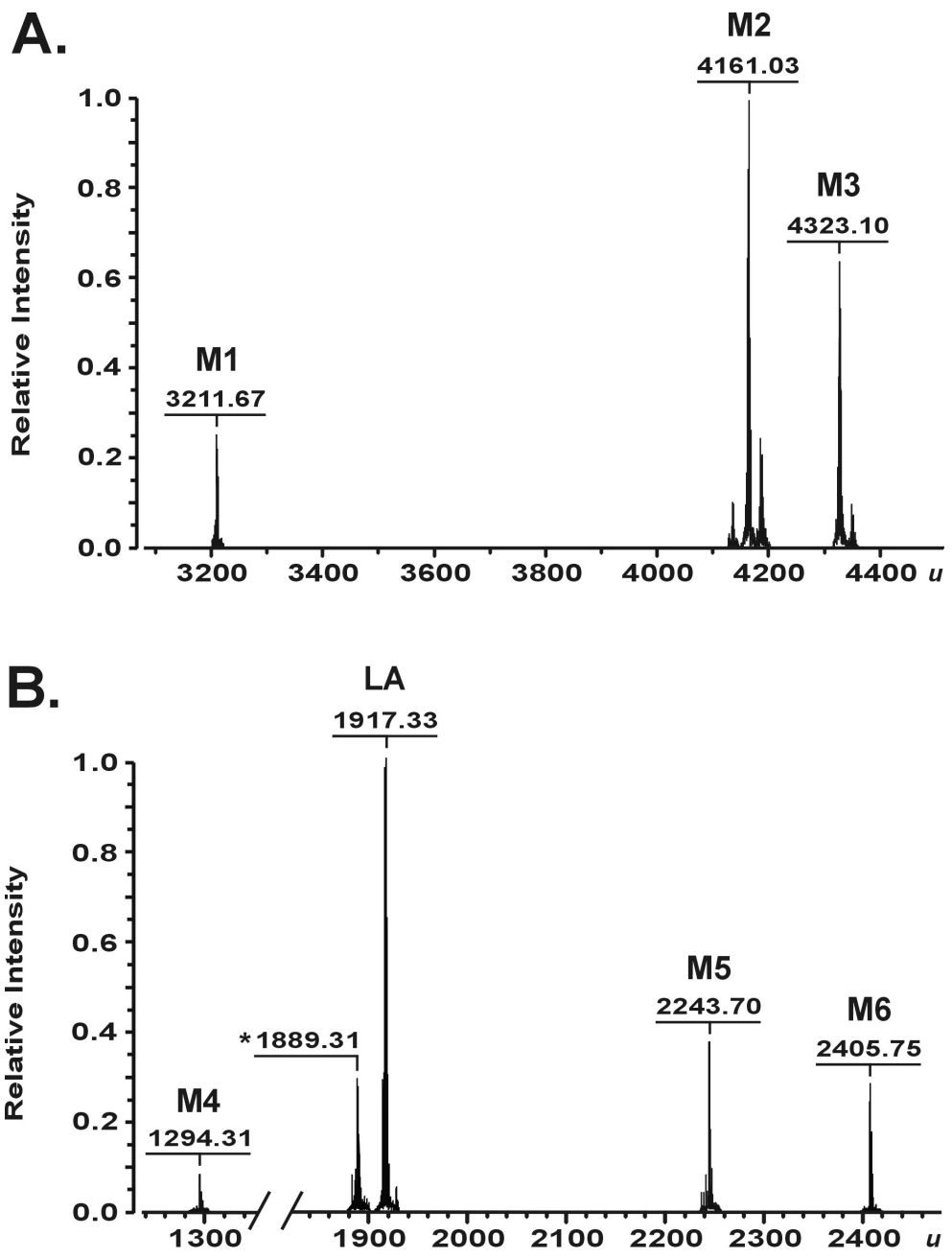

Supplementary Figure S2. Charge deconvoluted ESI FT-ICR mass spectra in negative ion mode of unligated LPS molecules from *A. aeolicus* recorded at a trap voltage of 5V (*A*) and after unspecific fragmentation in the collision cell at 30V (*B*). The peak assignments are listed in Table S2 of Supplemental Information. The peak at 1889.31 u is consistent with the structure of lipid A (LA; 1917.33 u) containing shorter acyl chain(s).

Supplementary Figure S3.

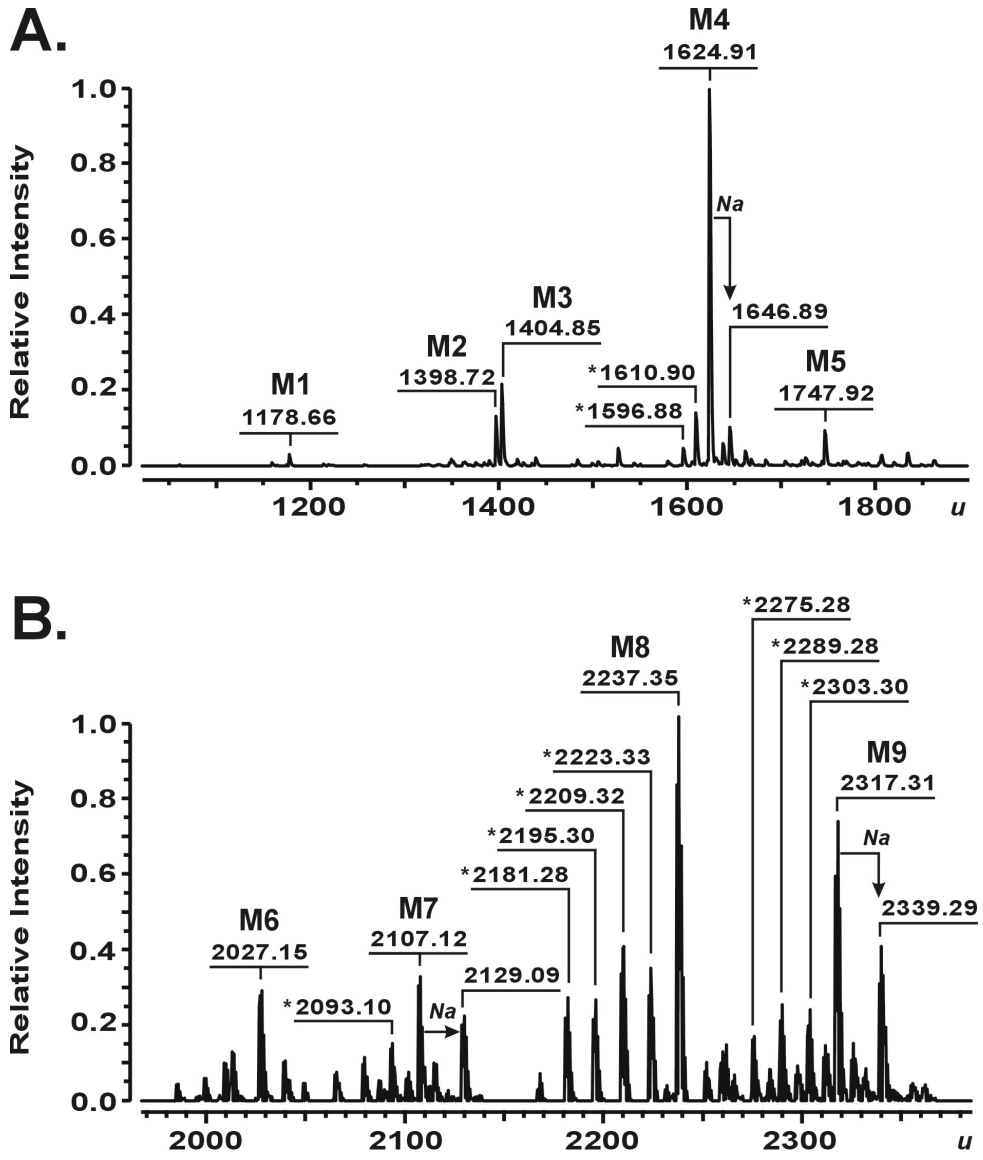

Supplementary Figure S3. Charge deconvoluted ESI FT-ICR mass spectra in negative ion mode of LPS molecules isolated from *E. coli* strains KPM123 (*A*) and KPM124 (*B*). The peak assignments are listed in Table S4 of Supplemental Information. Peaks presumably representing molecules with variations in acyl chain length are labeled with asterisks (Δm = 14.02 u). Triacylated molecular ions at 1178.66 u (M1) and 1398.72 u (M2) in panel *A* are likely artifacts produced during LPS isolation.

Supplementary Figure S4.

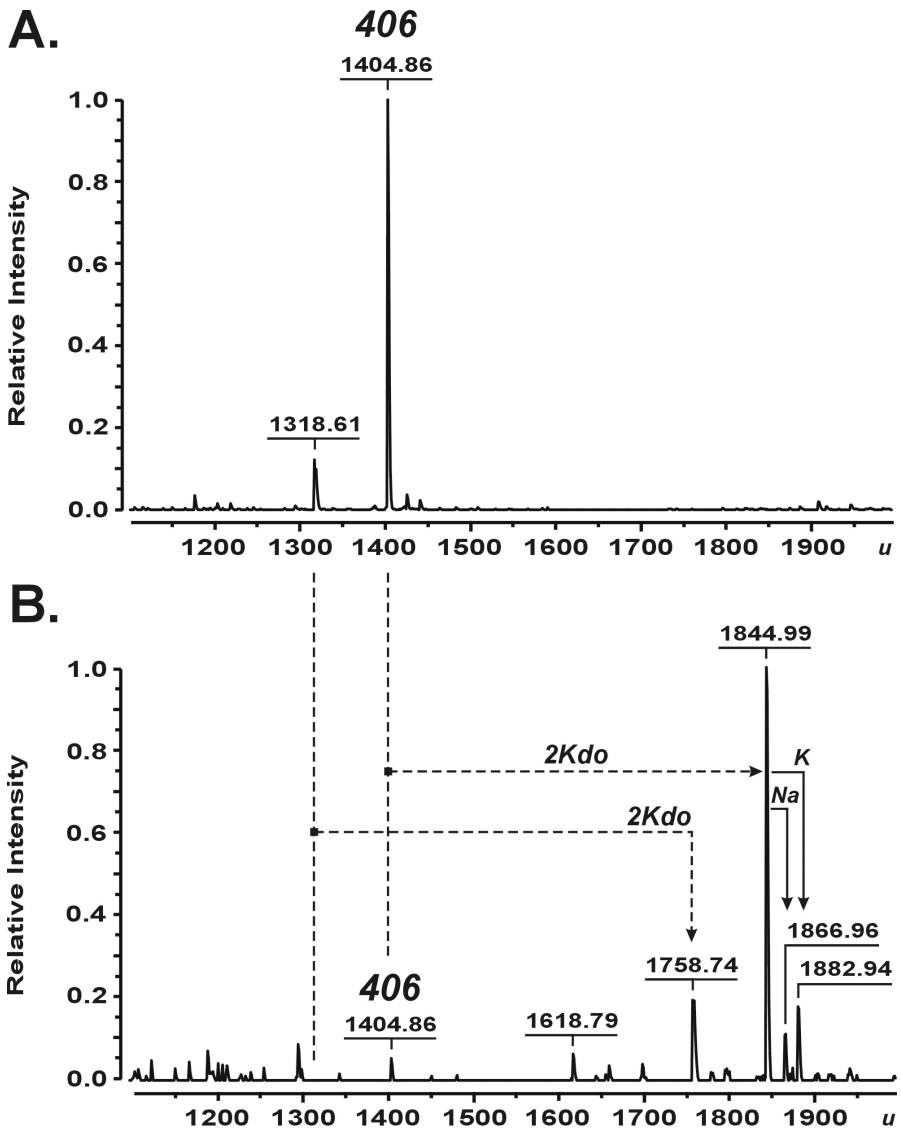

Supplementary Figure S4. Charge deconvoluted ESI FT-ICR mass spectra in negative ion mode showing the conversion of the tetraacyl-1,4′-bisphosphate lipid A precursor 406 (1404.86 u) (*A*) into Kdo_2-406 (1844.99 u) (*B*) by the Kdo transferase of *E. coli*. The reaction mixtures contained 100 mM HEPES, pH 7.5, 10% glycerol, 10 mM $MgCl_2$, 2 mM Kdo, 5 mM CTP, 3.2 mM Triton X-100, and 107 μM of compound 406. Incubation of the reactions was performed at 37 °C for 1 h with no enzymes (*A*), and in the presence of 17 milliunits of purified $KdsB_{ECO}$ and 75 μM of purified $WaaA_{ECO}$ (*B*). The peak at 1318.61 u (*A*) corresponds to a triacylated byproduct of 406 synthesis (see Figure 4) and was converted into a reaction product carrying two Kdo residues by $WaaA_{ECO}$ (1758.74 u) (*B*). The peak at 1618.79 u (*B*) presumably represents a triacylated degradation product of Kdo_2-406.

Supplementary Figure S5.

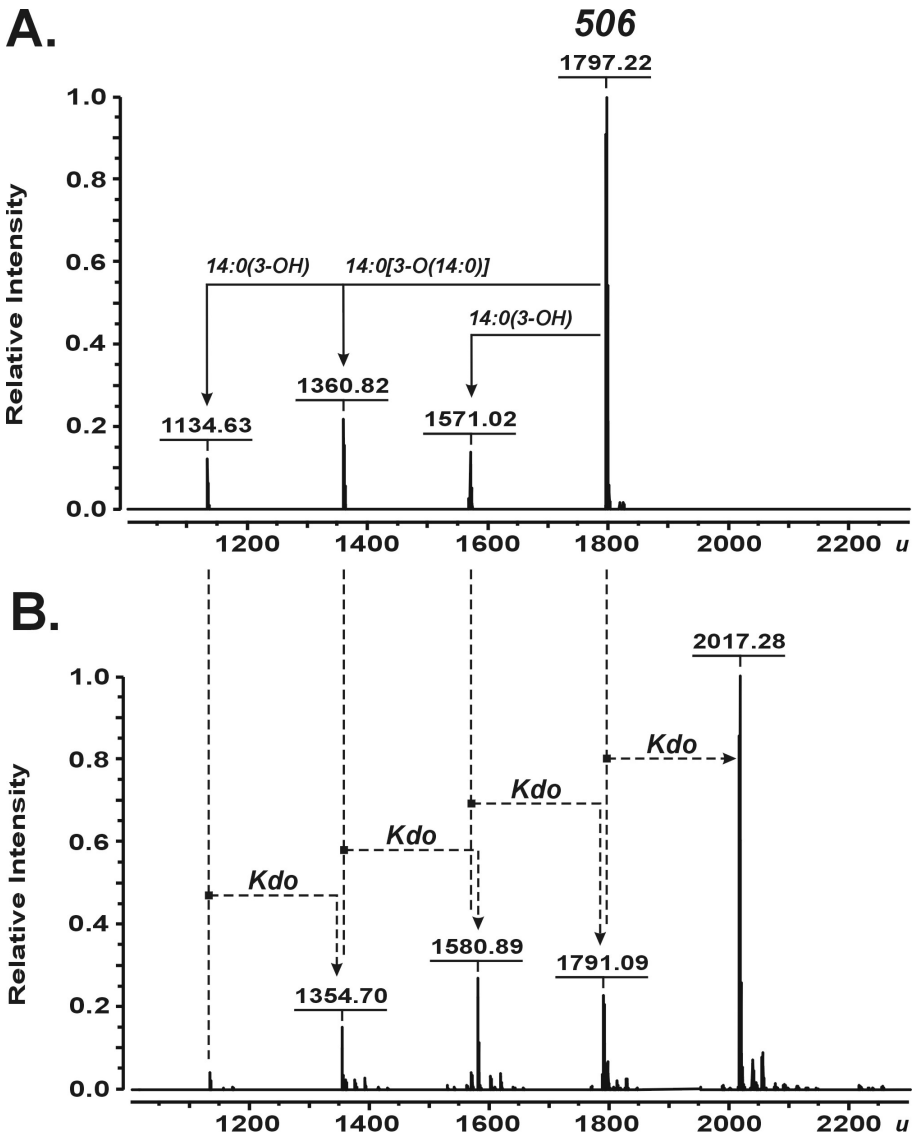

Supplementary Figure S5. Charge deconvoluted ESI FT-ICR mass spectra in negative ion mode demonstrating the $WaaA_{AAE}$-catalyzed conversion of the hexaacyl-1,4´-bisphosphate lipid A compound 506 (1797.22 u), as well as penta- (1571.02 u), tetra- (1360.82 u), and triacylated (1134.63 u) degradation products thereof (*A*) into reaction products carrying each a single Kdo residue (*B*). The structures of the differently acylated acceptor molecules are shown in Supplementary Figure S6. The reaction mixtures containing 100 mM HEPES, pH 7.5, 10% glycerol, 10 mM $MgCl_2$, 2 mM Kdo, 5 mM CTP, 3.2 mM Triton X-100, and 83 μM of the 506 mixture were incubated at 60 °C for 1 h with no enzymes (*A*), and in the presence of 17 milliunits of purified $KdsB_{AAE}$ and 75 μM of purified $WaaA_{AAE}$ (*B*).

Supplementary Figure S6.

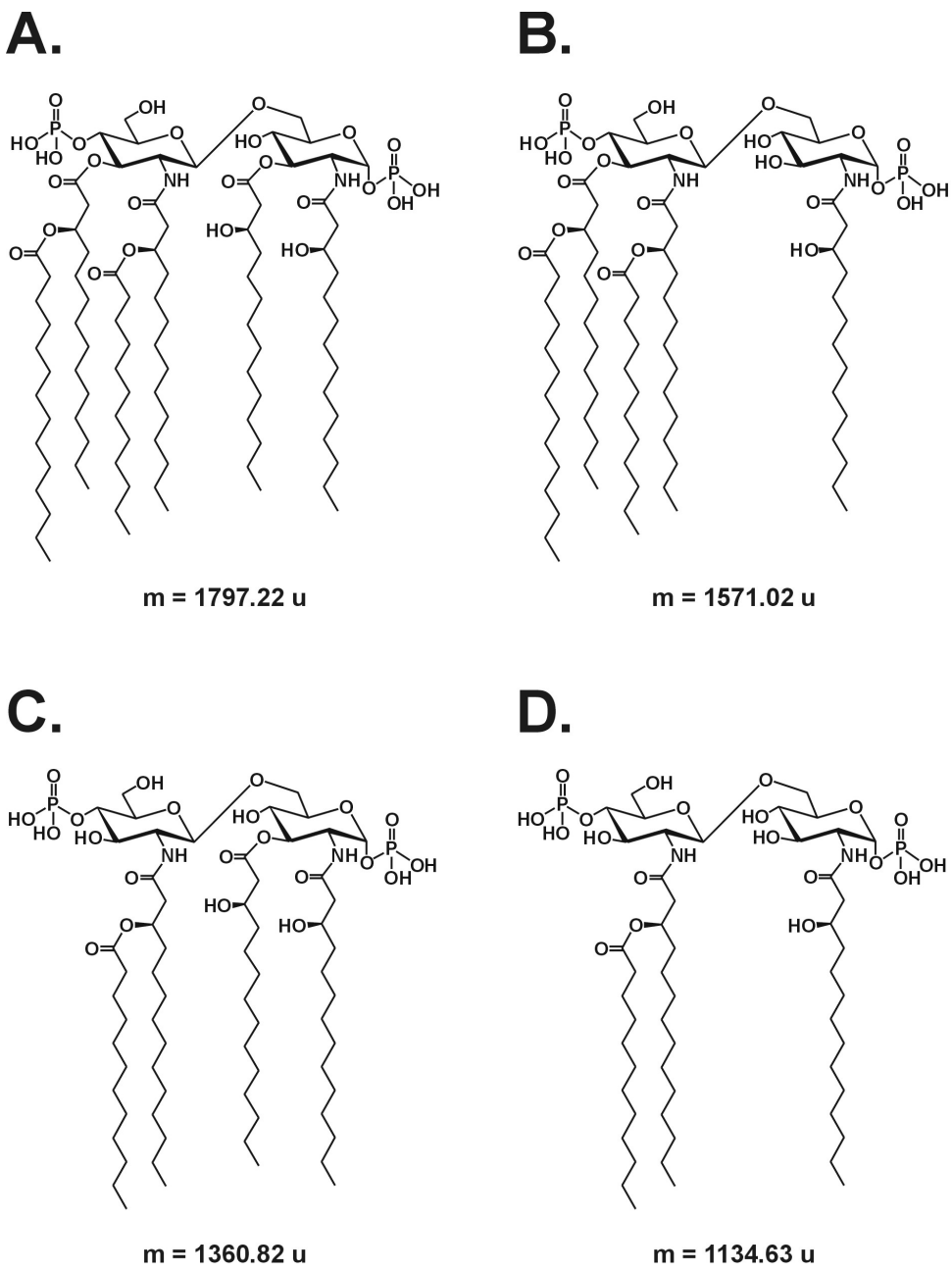

Supplementary Figure S6. Structures and molecular masses of the differently acylated lipid A molecules identified by ESI FT-ICR MS in compound 506 after long-term storage of the sample. The mass spectrum is shown in Supplementary Figure S5*A*.

Supplementary Figure S7.

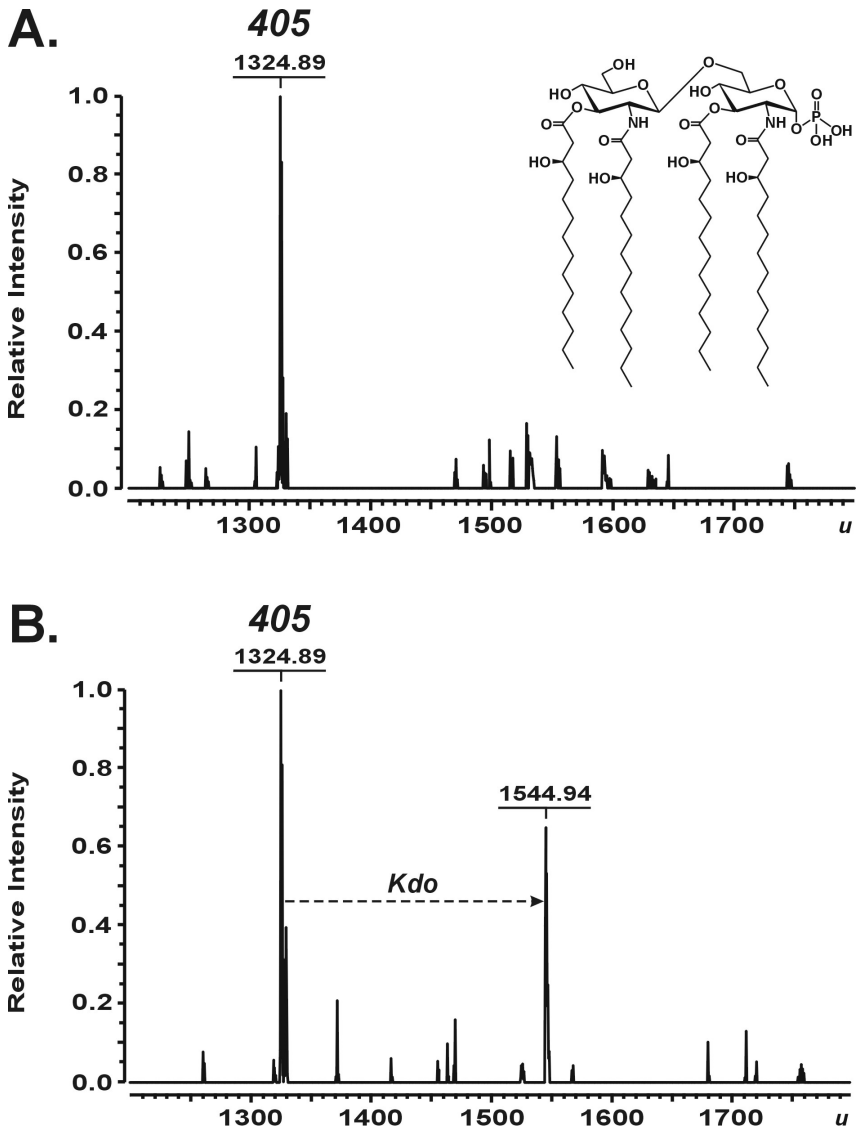

Supplementary Figure S7. Charge deconvoluted ESI FT-ICR mass spectra in negative ion mode showing the conversion of the tetraacyl-1-monophosphate lipid A precursor 405 (*inset* structure; 1324.89 u) (*A*) into Kdo-405 (1544.94 u) (*B*) by the Kdo transferase of *A. aeolicus*. The reaction mixtures containing 100 mM HEPES, pH 7.5, 10% glycerol, 10 mM $MgCl_2$, 2 mM Kdo, 5 mM CTP, 3.2 mM Triton X-100, and 113 μM of compound 405 were incubated at 60° C for 1 h with no enzymes (*A*), and in the presence of 17 milliunits of purified $KdsB_{AAE}$ and 75 μM of purified $WaaA_{AAE}$ (*B*).

Supplementary Figure S8.

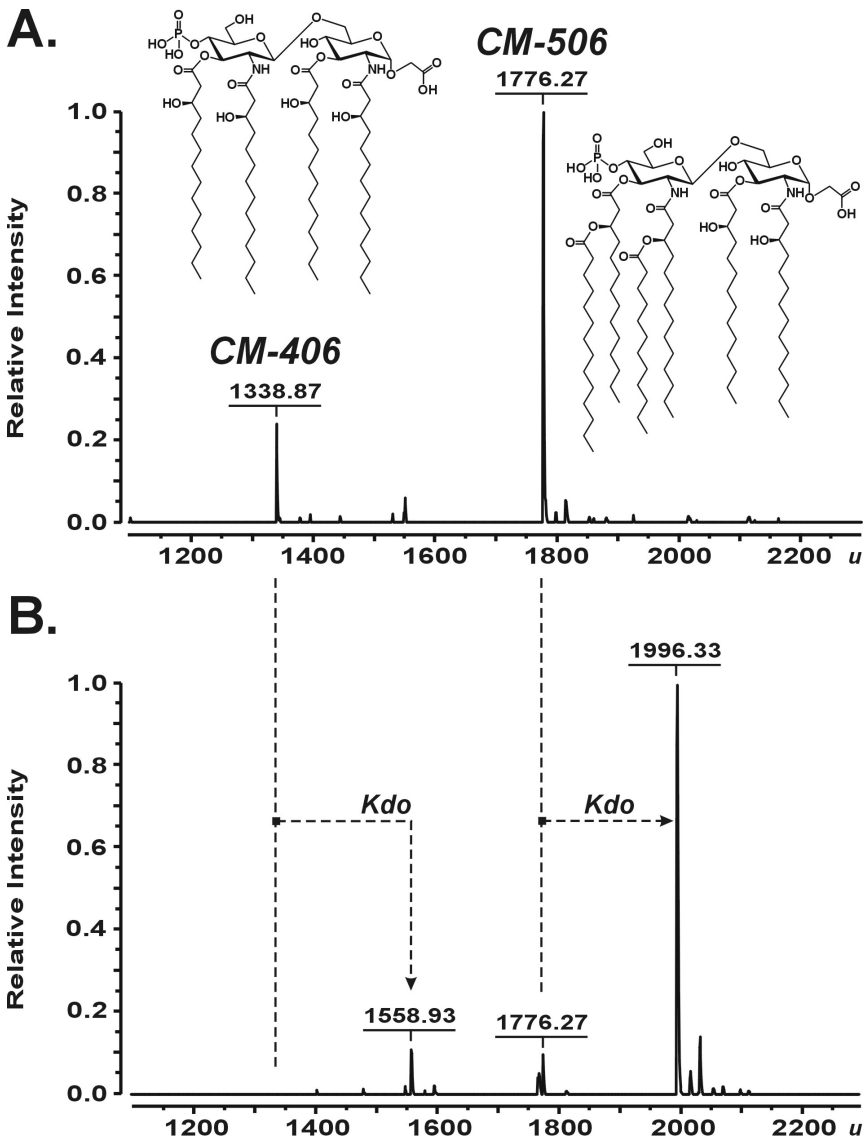

Supplementary Figure S8. Charge deconvoluted ESI FT-ICR mass spectra in negative ion mode demonstrating the $WaaA_{AAE}$-catalyzed conversion of the hexaacylated 1-carboxymethyl (CM) derivative CM-506 of lipid A (*inset* structure; 1776.27 u) and the 1-CM derivative CM-406 of the lipid A precursor 406 (*inset* structure; 1338.87 u) (*A*) into Kdo-CM-506 (1996.33 u) and Kdo-CM-406 (1558.93 u) (*B*), respectively. The reaction mixtures containing 100 mM HEPES, pH 7.5, 10% glycerol, 10 mM $MgCl_2$, 2 mM Kdo, 5 mM CTP, 3.2 mM Triton X-100, and 84 μM of the CM-506 sample were incubated at 60 °C for 1 h with no enzymes (*A*), and in the presence of 17 milliunits of purified $KdsB_{AAE}$ and 75 μM of purified $WaaA_{AAE}$ (*B*).

Supplementary Figure S9.

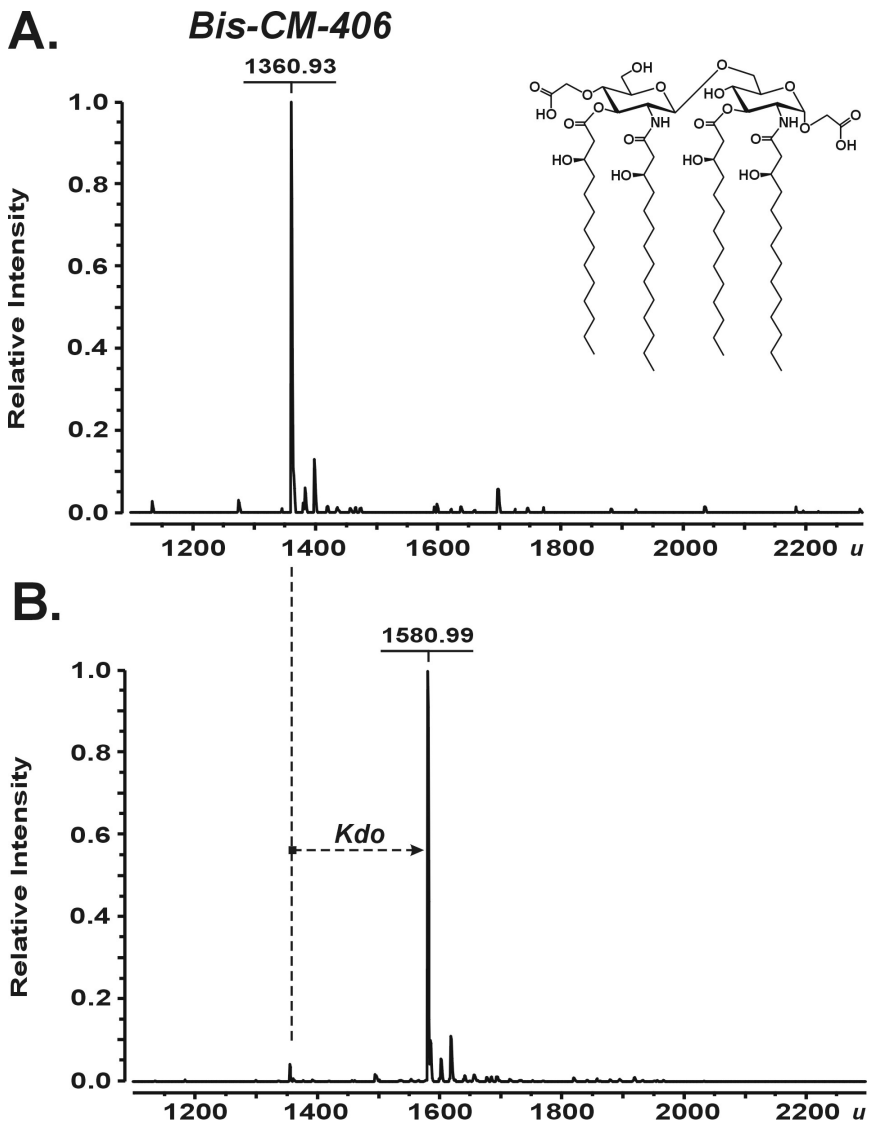

Supplementary Figure S9. Charge deconvoluted ESI FT-ICR mass spectra in negative ion mode showing the conversion of the tetraacyl-1,4′-CM compound Bis-CM-406 (*inset* structure; 1360.93 u) (*A*) into Kdo-Bis-CM-406 (1580.99 u) (*B*) by the Kdo transferase of *A. aeolicus*. The reaction mixtures containing 100 mM HEPES, pH 7.5, 10% glycerol, 10 mM $MgCl_2$, 2 mM Kdo, 5 mM CTP, 3.2 mM Triton X-100, and 110 μM of Bis-CM-406 were incubated at 60 °C for 1 h with no enzymes (*A*), and in the presence of 17 milliunits of purified $KdsB_{AAE}$ and 75 μM of purified $WaaA_{AAE}$ (*B*).

Supplementary Figure S10.

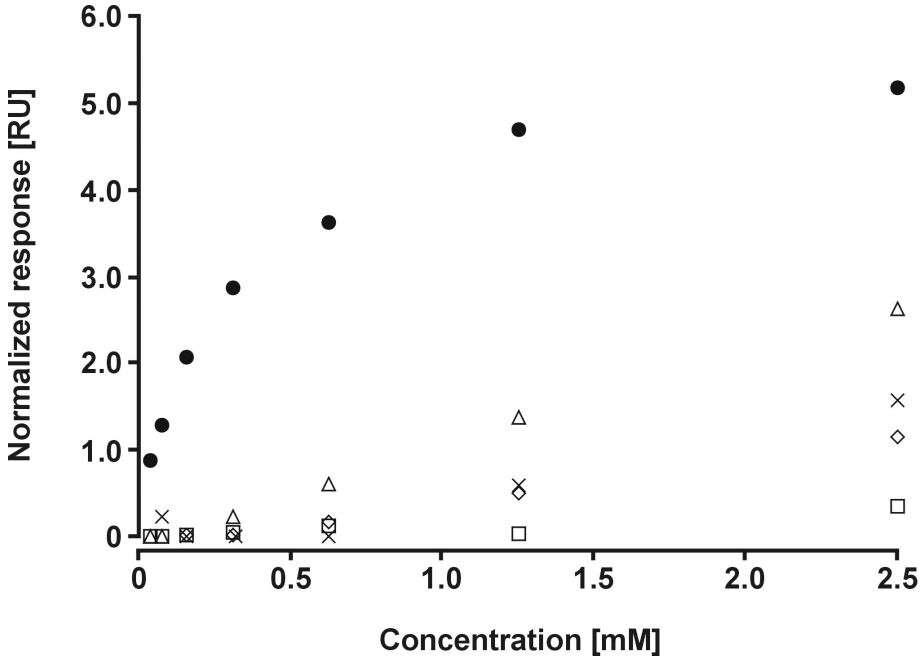

Supplementary Figure S10. Binding isotherms of the interaction between CMP (●), GMP (△), TMP (×), AMP (◇), and UMP (□) with the Kdo transferase of *A. aeolicus* immobilized to a CM5 sensor chip. The responses were normalized (normalized response = response*100/nucleotide-MW) for better comparison.

Supplementary Figure S11.

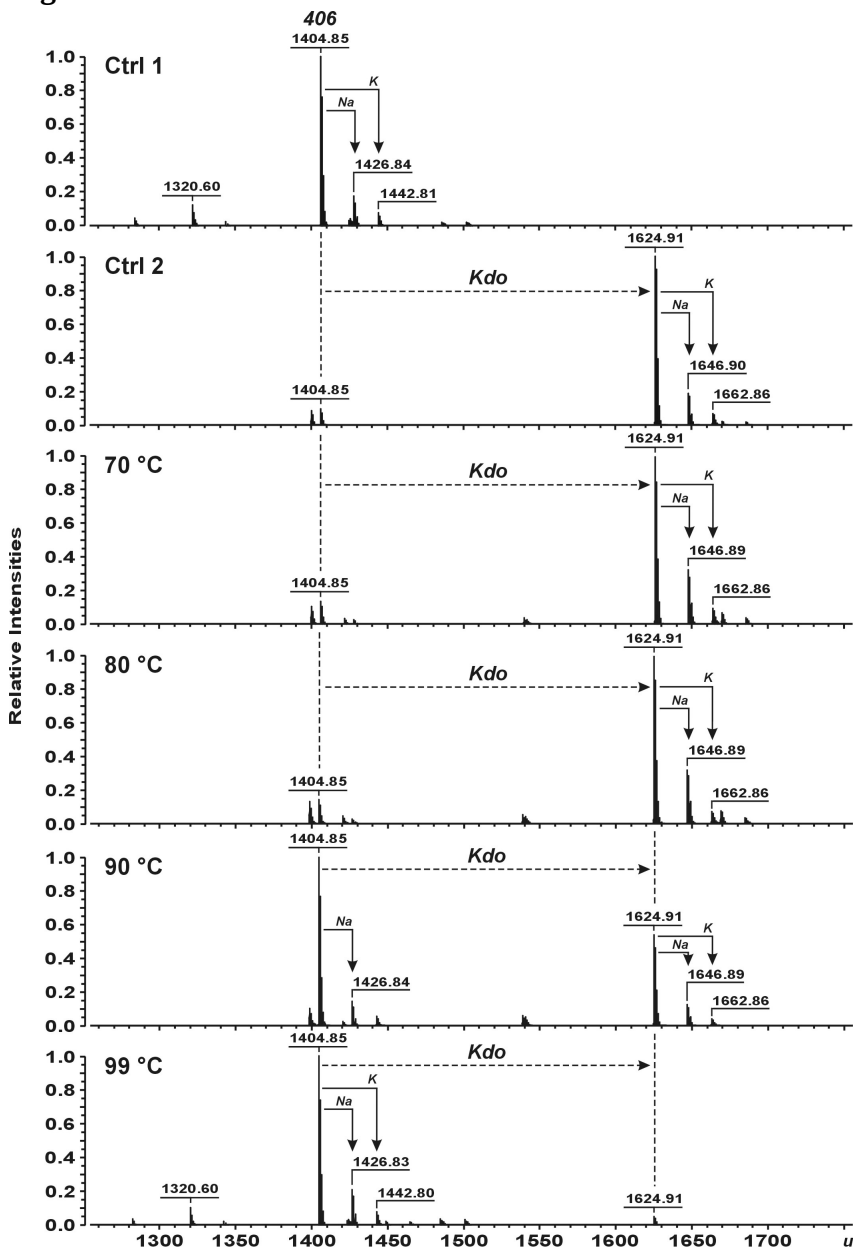

Supplementary Figure S11. Charge deconvoluted ESI FT-ICR mass spectra in negative ion mode demonstrating the $WaaA_{AAE}$-catalyzed conversion of the tetraacyl-1,4´-bisphosphate lipid A precursor 406 (1404.85 u) (*Ctrl1*) into Kdo-406 (1624.91 u) without (*Ctrl2*) and with treatment of the enzyme at the indicated temperatures for 1 h prior to the determination of residual activity. The activity was determined in reaction mixtures containing 100 mM HEPES, pH 7.5, 10% glycerol, 10 mM $MgCl_2$, 2 mM Kdo, 5 mM CTP, 3.2 mM Triton X-100, and 107 μM of compound 406. The reactions were incubated at 60 °C for 1 h with no enzymes (*Ctrl1*), and in the presence of 17 milliunits of purified $KdsB_{AAE}$ and 75 μM of either untreated (*Ctrl2*) or pre-treated $WaaA_{AAE}$. The peak at 1320.60 u originates from a batch-dependent byproduct of 406 synthesis.

Supplementary Figure S12.

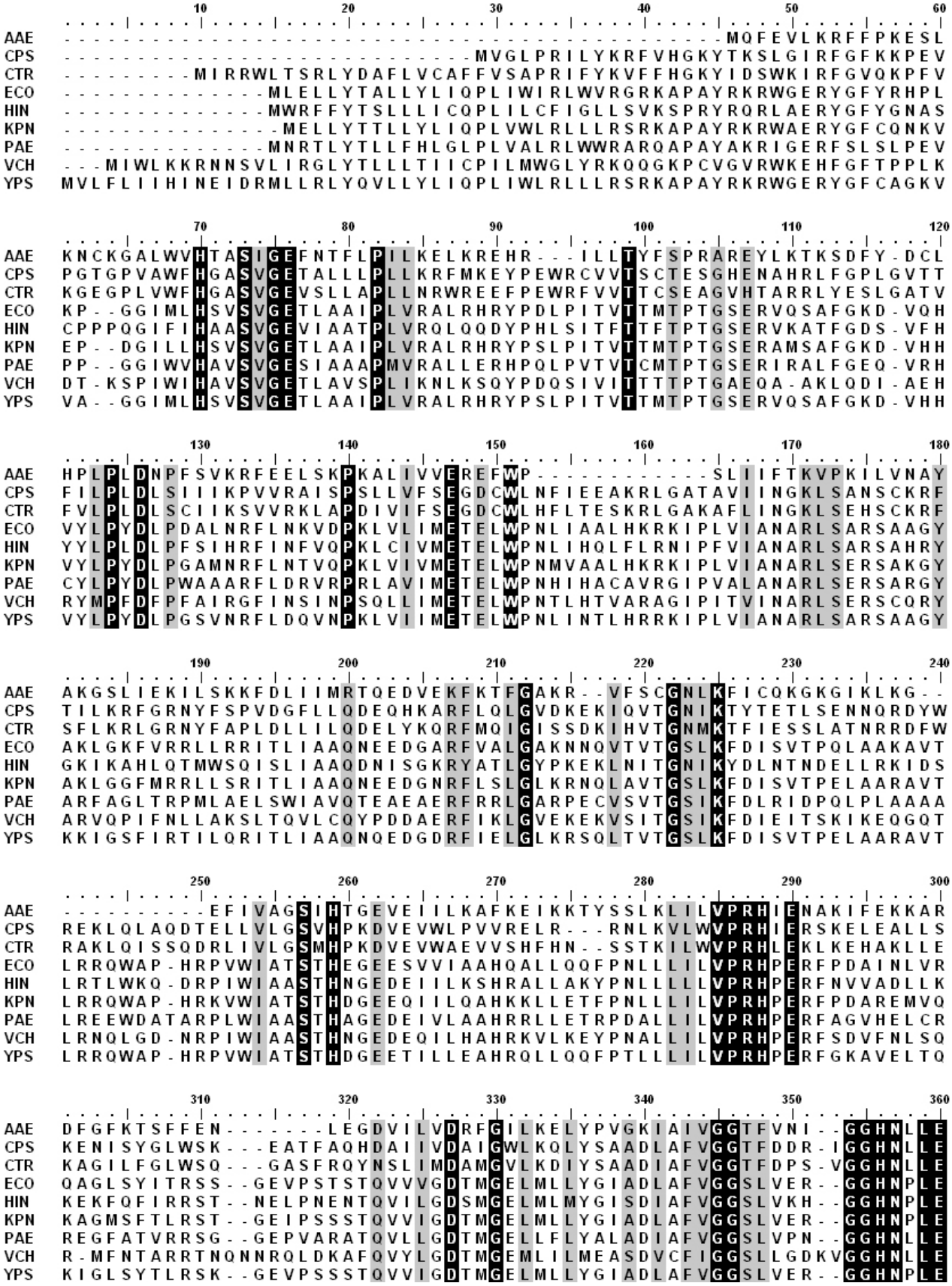

Supplementary Figure S12 - continued.

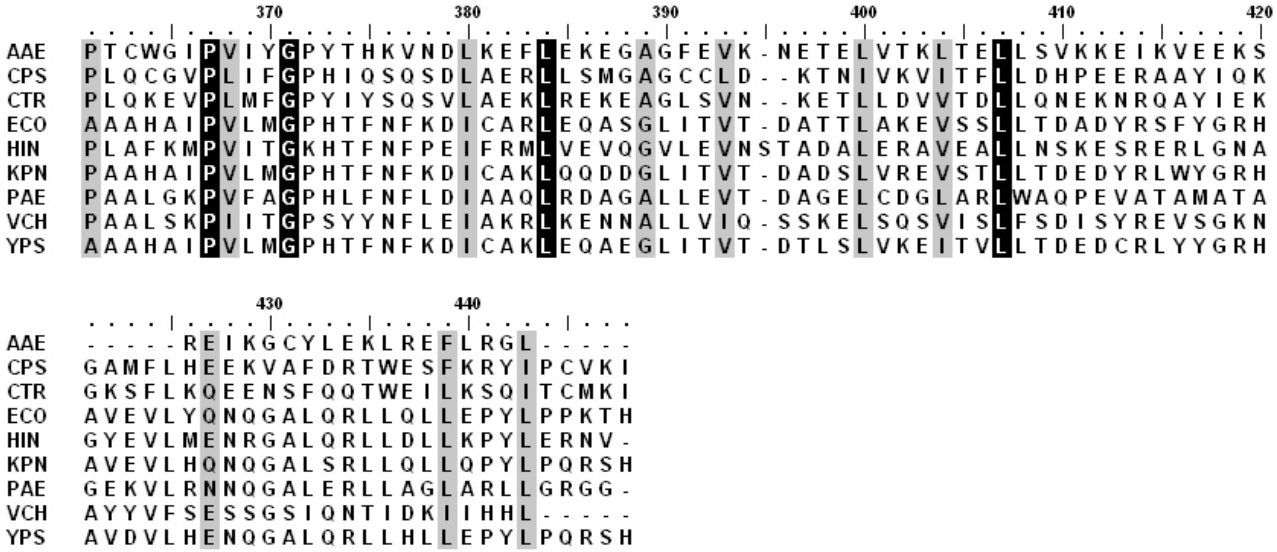

Supplementary Figure S12. Comparison of the deduced amino acid sequences of *waaA* genes using the PAM-250 scoring matrix for alignment. The single-letter code for amino acids is used. Dashes represent gaps introduced to optimize the alignment. Identical amino acids are shown in white on black and similar amino acids are shaded. The species names with accession numbers in parentheses are: AAE, *Aquifex aeolicus* VF5 (AAC06622); CPS, *Chlamydophila psittaci* 6BC (CAA49233); CTR, *Chlamydia trachomatis* (CAA80374); ECO, *Escherichia coli* K-12 substr. MG1655 (AAC76657); HIN, *Haemophilus influenzae* (P44806); KPN, *Klebsiella pneumoniae* subsp. *pneumoniae* MGH 78578 (ABR79357); PAE, *Pseudomonas seruginosa* PAO1 (AAG08373); VCH, *Vibrio cholerae* (AAL77371); YPS, *Yersinia pseudotuberculosis* YPIII (ACA70408).